TESLA-FEL-2006-11

Measurements of remanent fields in TQG quadrupoles by means of beam position measurements in FLASH

P. Castro, DESY

November 15, 2006

Abstract

A straight beam trajectory along the undulator section is mandatory for a high-gain FEL. Five pairs of quadrupoles of the so-called type TQG are installed between undulator segments in FLASH [1]. Quadrupoles are needed to increase the electron density and thus to increase the FEL gain. Measurements done on spare TQG quadrupoles [2] have shown remanent dipole fields with a (integrated) strength of up to 0.1 T·mm, which deflects a 500 MeV beam by about 60 μrad. Remanent fields vary in strength and direction from magnet to magnet and, therefore, they need to be measured at each magnet installed in FLASH.

Using relative beam position measurements, we have determined both horizontal and vertical components of the remanent dipole field for each individual quadrupole inside the undulator section. Here we present the method applied and the results obtained.

1 The undulator section in FLASH

A layout of the undulator section is shown in Fig. 1 indicating the name assigned to each component.

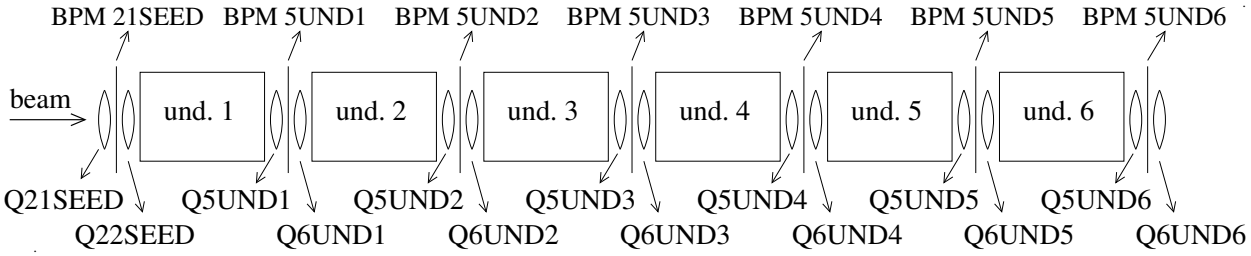

Figure 1: Schematic layout (not to scale) of the undulator system in FLASH. The electron beam enters from the left side. Quadrupole names begin with 'Q'. BPM stands for beam position monitor.

There are six undulator segments [3] numbered from 1 to 6, each with a length of 4.5 m. A pair of quadrupoles are located between the undulator segments as well as upstream

and downstream the undulator system. There is one beam position monitor (button type) between each pair of quadrupoles. All quadrupoles shown in Fig. 1 are of so-called type TQG (T stands for TTF or TESLA, Q for quadrupole). Quadrupoles are mounted on micromovers, which allows a precise positioning and alignment.

The quadrupole excitation current is provided by DC power supplies that deliver any requested value between +100 A and −100 A. Quadrupoles Q21SEED, Q22SEED, Q5UND6 and Q6UND6 have each an independent power supply. One power supply is connected to the "Q5 quadrupoles" (Q5UND1, Q5UND2, Q5UND3, Q5UND4 and Q5UND5) in series and a second power supply is connected to the "Q6 quadrupoles" (Q6UND1, Q6UND2, Q6UND3, Q6UND4 and Q6UND5). An additional AC power supply, used as degausser, is connected via relays to the Q5 and Q6 quadrupoles.

In this paper we use the sign convention that on the horizontal plane the positive direction goes to the right looking downstream (in the direction of the beam) and on the vertical plane the positive direction goes upwards. The convention for quadrupole currents is that a positive current induces a horizontal focusing quadrupole field.

2 Description of the method applied

Here we describe the procedure to measure the relative beam deflection caused by remanent dipole fields between the following three cases:

- after degaussing with the AC power supply
- after applying a DC current of +100 A
- and after applying a DC current of −100 A.

The method described in the following is independent of BPM calibrations, optics and relative misalignments. The error contributions are discussed in detail in Sec. 7. In preparation for the measurement, we have degaussed all Q5 and Q6 quadrupoles inside the undulator section to reduce the magnetic fields to a minimum bias. Then, we have applied first +100 A and then 0 A to the five Q5 quadrupoles. With this we have a remanent quadrupole field in Q5 quadrupoles which can be used for steering the beam position by using the quadrupole micromovers. In order to get the beam through the undulator, the optics upstream is adjusted.

With Q5 quadrupoles with remanent quadrupole field (for beam steering purpose), the measurement of the remanent dipole field of Q6 quadrupoles consist of, first, recording as reference the beam position with the BPMs along the undulator. Second, the five Q6 quadrupoles, which are connected in series, are set to +100 A and then to a current that approximately compensates the remanent quadrupole field (see Sec. 4). Thus, the beam position change observed is only due to a remanent dipole field B (different for each quadrupole) that deflects the beam with angles x'_{Q6} and y'_{Q6}. Finally, the beam position is corrected back to the reference position using the horizontal and vertical movers of Q5 quadrupoles. That is, the relative change in beam position measured at BPM 5UND2 is corrected using quadrupole Q5UND1, the change at BPM 5UND3 is corrected with Q5UND2, and so on,

proceeding downstream. The resulting quadrupole displacements Δx_{Q5} and Δy_{Q5} deflect the beam with angles x'_{Q5} and y'_{Q5} that are approximately equal in amplitude to x'_{Q6} and y'_{Q6}, respectively, and therefore

$$B_y \simeq g_{rem} \cdot \Delta x_{Q5} \quad , \quad B_x \simeq g_{rem} \cdot \Delta y_{Q5} \tag{1}$$

where g_{rem} is the remanent field gradient of Q5 quadrupole. Again, we apply the same procedure after setting Q6 quadrupole to a current of -100 A and then to a current that compensates the remanent quadrupole field.

In order to measure the beam deflection introduced by remanent dipole fields in Q5 quadrupoles, we have degaussed all quadrupoles and have applied the same method described above with exchanging the words "Q5" and "Q6".

3 Results

We have applied the method described in Sec. 2 to measure the relative beam deflection due to remanent dipole fields created after setting +100 A (and created after setting −100 A) compared to the bias field after degaussing. The relative quadrupole displacements applied to compensate the remanent dipole fields in each case are listed in Table 1. The RMS (root mean square) of all the values is 0.26 mm. Statistically, there is no difference between the horizontal and the vertical plane. The largest beam deflection observed is due to quadrupole Q6UND5.

	Δx_Q **[mm]**		Δy_Q **[mm]**	
last I	+100 A	−100 A	+100 A	−100 A
Q5UND1	−0.06	−0.03	0.0	0.02
Q6UND1	−0.01	0.05	0.02	0.02
Q5UND2	−0.30	0.43	0.20	−0.24
Q6UND2	0.18	−0.16	0.12	−0.09
Q5UND3	0.0	0.0	0.10	−0.01
Q6UND3	0.34	−0.35	0.17	−0.31
Q5UND4	−0.11	−0.07	−0.31	0.30
Q6UND4	0.10	−0.01	−0.41	0.45
Q5UND5	0.14	0.04	0.0*	0.21
Q6UND5	−0.62	0.64	−0.40	0.46
RMS	0.26	0.27	0.24	0.27

Table 1: Relative quadrupole displacement needed to compensate the beam deflection after setting +100 A (and after setting −100 A) compared with the bias field after degaussing. (*:Quadrupole mover at the limit of the permissible range, impeding an orbit corretion at the downstream BPM.)

The magnitude of the corresponding remanent dipole fields is calculated in Sec. 5 by applying Eq. (1). For this we need to know the value of g_{rem}, which is presented in Sec. 4.

4 Remanent quadrupole gradient measurements

To perform the measurements described in Sec. 2, we need to know the remanent quadrupole gradient g_{rem} and the current needed to compensate this remanent field. Measurements of the integrated quadrupole gradient as function of the quadrupoles current made by Y. Holler on a spare quadrupole are shown in Fig. 2. A linear fit to the data points taken between -10 A and 10 A yields the equation

$$\int g dz = G_0 + G_1 \cdot I \tag{2}$$

where I is the quadrupole current, $G_0 = \int g_{rem} dz = 76$ mT and $G_1 = 85$ mT/A. Thus, the current needed to compensate the remanent field is $G_0/G_1 = -0.89$ A. This last value is in disagreement with results obtained from beam position measurements (described in the following).

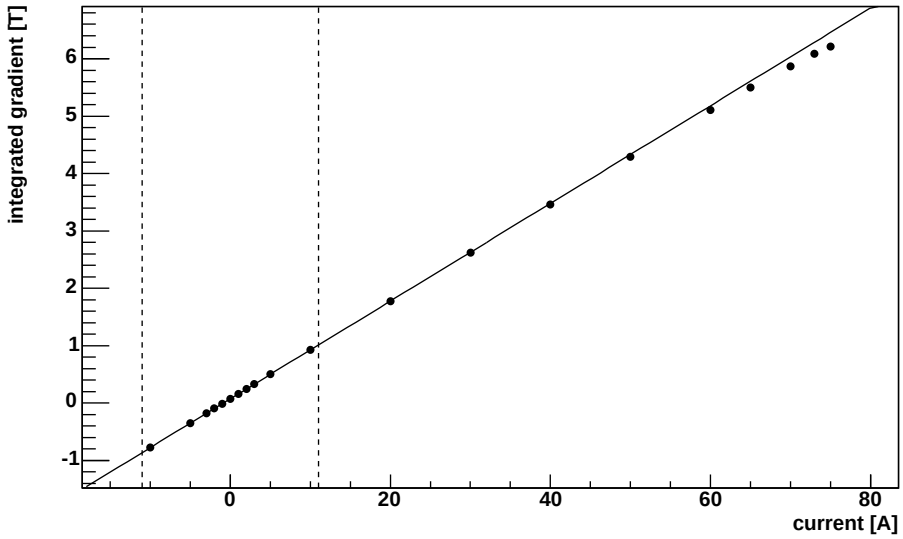

Figure 2: Integrated gradient as function of the quadrupole excitation current starting at +75 A and descending. These measurements are carried out by Y. Holler on spare quadrupole TQG with serial number 18. Vertical dashed lines indicate the range of points included in the linear fit (full line) of Eq. (2).

The beam deflection change $\Delta x'_Q$ due to a quadrupole displacement Δx_Q is given in thin lens approximation by

$$\Delta x'_Q = c \cdot e \cdot \Delta x_Q \cdot \frac{\int g dz}{E} \tag{3}$$

where g is the quadrupole gradient, E is the particle energy, c is the light velocity in vacuum and e is the electron charge. The change in beam position Δx_B at a BPM downstream is given by

$$\Delta x_B = R_{12} \Delta x'_Q \tag{4}$$

where R_{12} is the second element of the transfer matrix between the quadrupole and the BPM.

We have analyzed beam position measurements taken with BPMs along the undulator section (and downstream) as function of quadrupole position and quadrupole current. An example of such measurements for quadrupole Q6UND1 is shown in Fig. 3. First of all, the quadrupole current is set to +100 A and then to zero. Then, beam position measurements are taken with BPM 5UND2 for a quadrupole current of 0, −0.5, −1.5, −2 and −3 A, in this order. For each current the quadrupole position has been varied between −0.8 and 0.6 mm horizontally. The scattering of the data points in Fig. 3 is due mainly to BPM noise and to beam position jitter.

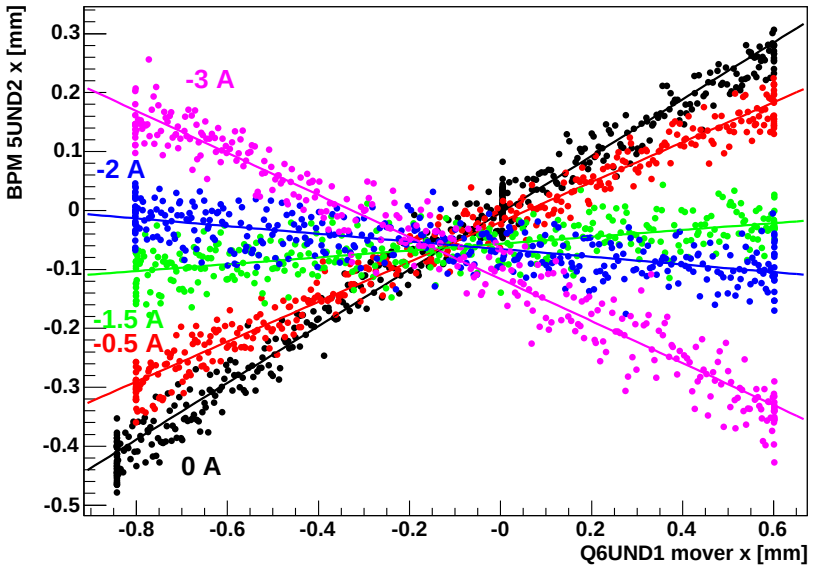

Figure 3: Horizontal beam position measured with BPM 5UND2 as function of position and current of quadrupole Q6UND1. One line is fitted to the measurement points taken with the same current.

We have fitted one line to the measurement points taken with the same current. The slope of each line (defined as fit parameter a_1) corresponds to the ratio between beam position change at the BPM, as given by Eq. (4), and the quadrupole position change in Eq. (3)

$$a_1 = \frac{\Delta x_B}{\Delta x_Q} = c \cdot e \cdot R_{12} \cdot \frac{\int g dz}{E} \tag{5}$$

which can be written using parameters G_0 and G_1 from Eq. (2) as

$$a_1 = P_0 + P_1 \cdot I \tag{6}$$

where $P_0 = c \cdot e \cdot R_{12} \cdot G_0/E$ and $P_1 = c \cdot e \cdot R_{12} \cdot G_1/E$.

The parameter a_1 of each linear fit is plotted as a function of the quadrupole current in Fig. 4. A linear fit to the points in Fig. 4 gives the values $P_0 = 0.48$ and $P_1 = 0.28$ A^{-1} for Eq. (6). The value $P_0/P_1 = G_0/G_1 = -1.73$ A (for this example) corresponds to the compensation current for the remanent quadrupole field. This result is independent of R_{12},

therefore, it is independent of optics errors in the lattice between the quadrupole and the BPM. It is also independent of scaling errors of quadrupole position and is independent of BPM calibrations. In fact, one can choose any BPM downstream the quadrupole to get a similar plot of a_1 versus quadrupole current I.

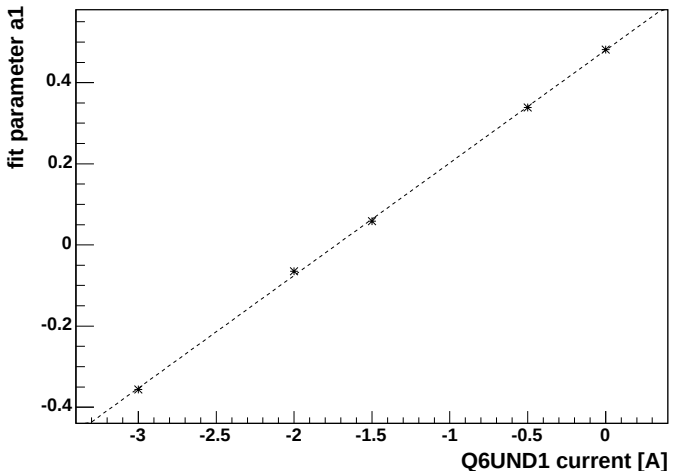

Figure 4: Fit parameter a_1 (from Fig. 3) as function of quadrupole current for Q6UND6. A linear fit is shown with a dashed line.

We proceed as described in the previous example with data obtained using other quadrupoles in both horizontal and vertical planes. For some quadrupoles, several values are obtained by using different downstream BPMs for both planes. All the values for the remanent compensation current are shown in Fig. 5.

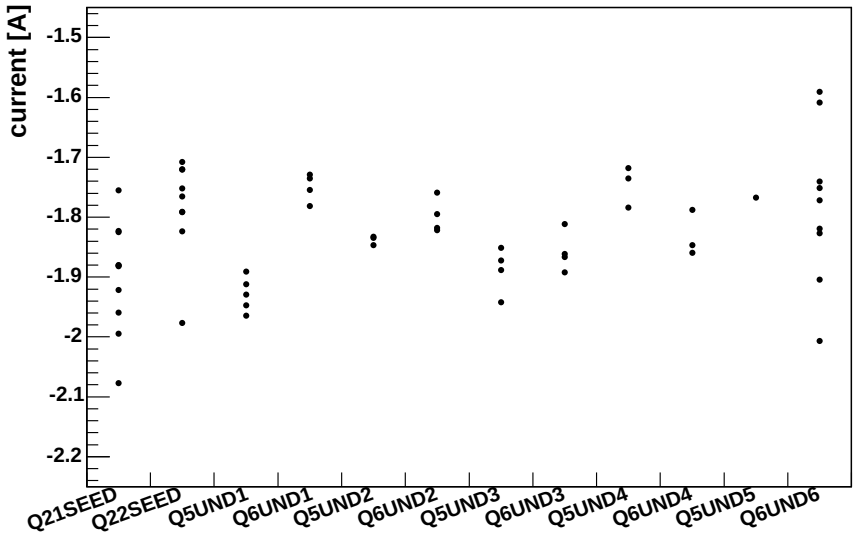

Figure 5: Current that compensates the remanent quadrupole field of quadrupoles TQG installed in the undulator section.

The spread of these results serves as an estimation of the statistical accuracy of this method. The spread of these results per quadrupole have a typical standard deviation of 0.03 A with the exception of Q21SEED, Q22SEED and Q6UND6 that have a standard deviation of 0.1 A. Taking all these points, the mean value of the compensation current is -1.82 A. The standard deviation of the mean value from each quadrupole is 0.06 A. This result differs from the compensation current of -0.89 A obtained from magnetic measurements of spare quadrupole, see Eq. (2). The reason of this disagreement is not yet understood.

The calculation of G_1 from parameter P_1 of Eq. (6) depends, however, from the optics parameter R_{12}. In the case of the example shown in Fig. 4, the value of R_{12} between Q6UND1 and BPM 5UND2 can be approximated by the longitudinal distance of 4.9 m. For a beam energy of 500 MeV we have $G_1 = 95$ mT/A (for this example).

We proceed similarly with the other quadrupoles, selecting the data from the BPM just downstream the quadrupole selected. In this case and only for the horizontal plane, we can approximate R_{12} by the distance between the BPM and the quadrupole, which is 5.3 m for Q5 quadrupoles and 4.9 m for Q6 quadrupoles. The results are shown in Fig. 6. The average is 85 mT/A which is fully in agreement with the value obtained from magnetic measurements on a spare quadrupole, see Eq. (2). The standard deviation of the values is 11 mT/A, which is a 13% of the absolute value of G_1, probably due to systematic errors on relative calibration of BPMs, on relative calibration of quadrupole position sensors, etc.

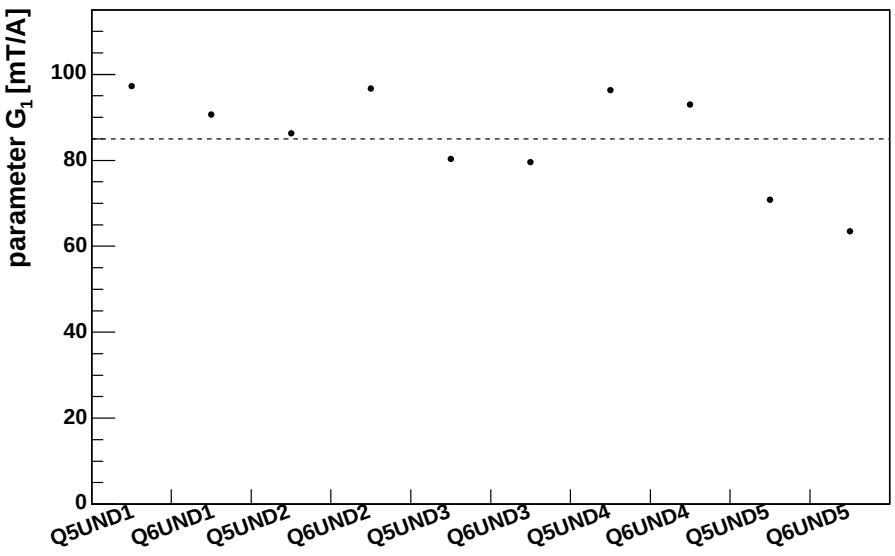

Figure 6: Parameter G_1 from Eq. (6) of quadrupoles TQG installed in the undulator section. The horizontal dashed line indicates the value obtained from magnetic measurements on a spare quadrupole.

Based on these results obtained from beam position measurements, we have chosen a remanent compensation current of -1.8 A and the values of $G_0 = 155$ mT and $G_1 = 85$ mT/A for Eq. (2).

5 Measured dipole fields

Using the value $G_0 = 155$ mT obtained in Sec. 4 for the integrated remanent gradient we apply the results listed in Table 1 to Eq. (1) for integrated fields

$$\int B_y dz \simeq G_0 \cdot \Delta x_Q \quad , \quad \int B_x dz \simeq G_0 \cdot \Delta y_Q \tag{7}$$

to obtain the integrated remanent field $\int \vec{B} dz = (\int B_x dz, \int B_y dz)$ of quadrupoles in the undulator section. The results are shown in Fig. 7.

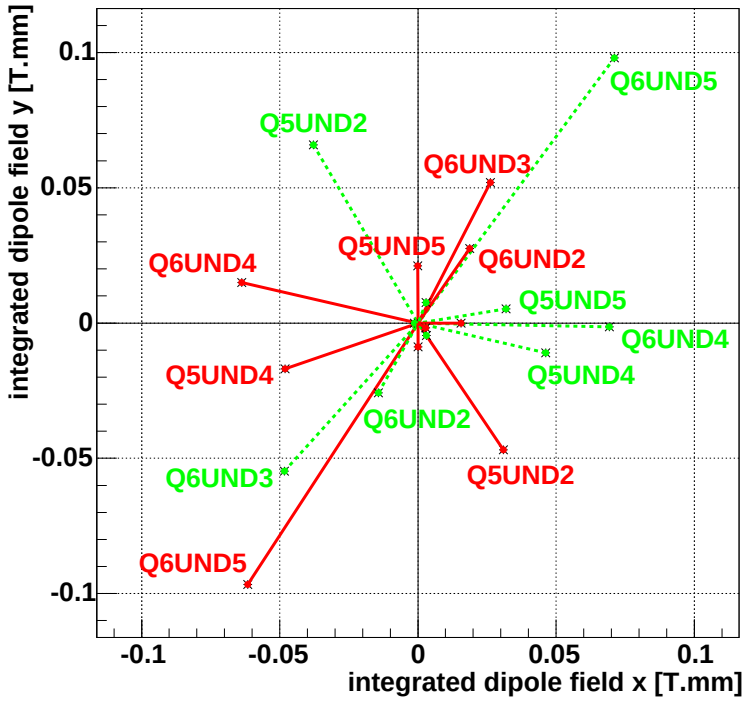

Figure 7: Integrated remanent dipole field of the quadrupoles listed in Table 1. With red color and full lines: after setting +100 A and with green color and dashed lines: after setting −100 A. Note the same scale for both planes.

The total amplitude A of the integrated remanent dipole is calculated from its horizontal and vertical components

$$A = \sqrt{\left(\int B_x dz\right)^2 + \left(\int B_y dz\right)^2}$$

The largest value of the total amplitude is 0.11 T·mm in quadrupole Q6UND5 and the RMS of the total amplitude of all 10 quadrupoles is 0.08 T·mm .

6 Trajectory error due to remanent dipole fields

The beam position error introduced by the remanent dipole fields of the quadrupoles in the undulator section depends on the optics. In the simplest case that all quadrupole gradients

are zero (that is, all quadrupoles are set to +100 A and then to −1.8 A) and assuming the beam is on axis at the entrance of the undulator, the horizontal beam offset at the end of the undulator is about 0.17 mm for a beam energy of 500 MeV as it is shown in Fig. 8. It is just a coincidence that the beam position displacement due to Q5 quadrupoles roughly compensates the displacement caused by Q6 quadrupoles.

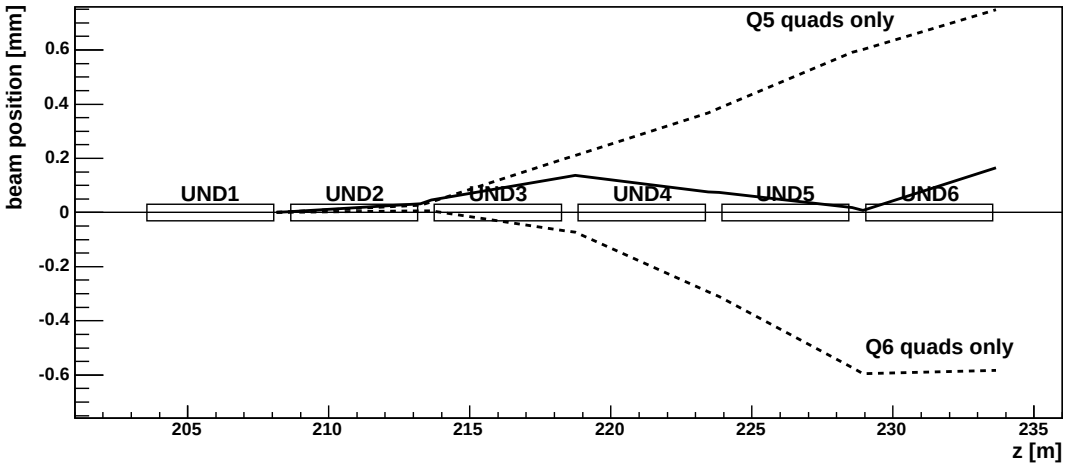

Figure 8: Simulation of the horizontal beam position error along the undulator section due to remanent dipole fields of Q5 quadrupoles and Q6 quadrupoles (dashed lines) and both together (full line) assuming that the quadrupole gradients are zero.

For nominal optics, the net focusing effect of the quadrupoles reduces the amplitude of the beam displacement introduced by remanent dipole fields. The result of a simulation of the horizontal beam trajectory along the undulator section for the so-called "variant 1" optics (with 130° phase advance per undulator segment) is shown in Fig. 9.

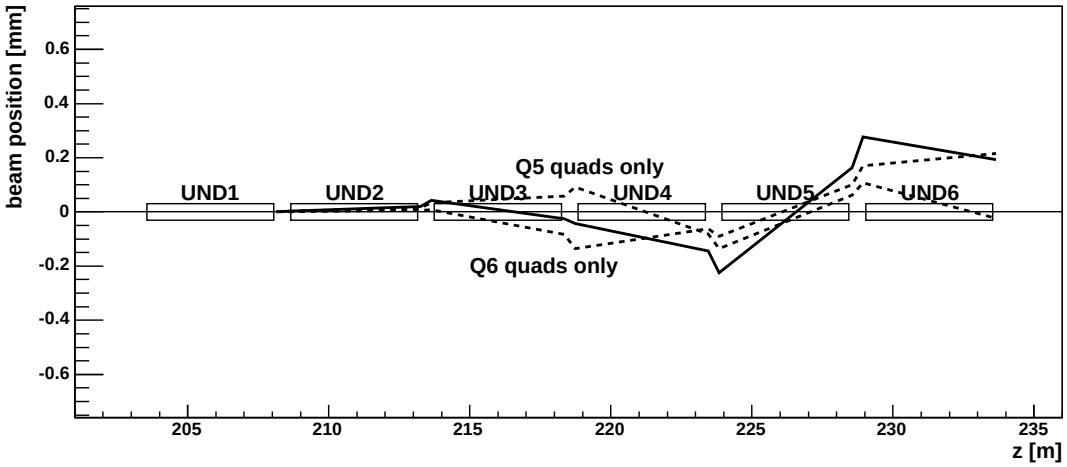

Figure 9: Simulation of the horizontal beam position error along the undulator section due to remanent dipole fields of Q5 quadrupoles and Q6 quadrupoles (dashed lines) and both together (full line) assuming quadrupole gradients corresponding to the "variant 1" optics [4].

In general, the beam displacement depends on the value of the betatron function at the quadrupoles (which is about 5 m in average) and the phase advance between them (which varies from 50° to 130° from one optics version to another [4]). Statistically, the expected orbit displacement after N random dipole field errors is [5]

$$\sigma_x =< \beta > \sqrt{N}\sigma_\theta \tag{8}$$

where $< \beta >$ is the average value of the betatron function at the quadrupoles and BPMs. σ_θ is the RMS of the beam deflection due to random dipole field errors σ_B=0.08 T·mm (Sec. 5) and it is given by

$$\sigma_\theta = c \cdot e \cdot \frac{\sigma_B}{E}$$

which is about 50 μrad for a beam energy of 500 MeV. Using Eq. (8), the expected RMS position displacement at the end of the undulator is 0.75 mm.

7 Error contributions

Correcting the beam position to a reference position (as described in Sec. 2) has the advantage that the results are independent of calibration errors in BPMs and of optics errors in the undulator lattice. However, there is a systematic error due to the difference of longitudinal position z between quadrupole Q5 and Q6. The beam position change Δx_B observed at the downstream BPM (at position z_B) due to the pure remanent dipole field[1] of a Q6 quadrupole is

$$\Delta x_B = x'_{Q6}(z_B - z_{Q6})$$

and is compensated by the displacement of the adjacent Q5 quadrupole that has a quadrupole field

$$\Delta x_B = x'_{Q5}(z_B - z_{Q5})$$

The beam deflection due to the remanent dipole field of Q6 quadrupoles is underestimated by

$$\frac{x'_{Q6} - x'_{Q5}}{x'_{Q6}} = \frac{z_{Q6} - z_{Q5}}{z_B - z_{Q5}} \simeq \frac{0.4 \text{ m}}{5 \text{ m}} \simeq 8\%$$

Similarly, the deflection of a pure remanent dipole field of Q5 quadrupole is overestimated by approximately 8% if it is compensated with a displacement of Q6 quadrupole with a quadrupole field.

In order to get rid of this systematic error, an alternative procedure is to excite some quadrupole field in the same quadrupole at which we want to measure the remanent dipole field. It is then required that the beam is centered in the quadrupole, otherwise the quadrupole field will also deflect the beam and introduce an error in the measurement. This procedure requires a precise knowledge of the quadrupole center with respect to the BPM and a good scale calibration and good linearity response of the BPM. We have opted not to

[1] the deflection of a pure dipole field is independent of the magnet position

use this alternative procedure, since the results from quadrupole-to-BPM alignment are at present neither reliable nor accurate enough.

Other sources of systematic errors are scaling errors from quadrupole position sensors (see Sec. 8) and the determination of the remanent gradient field (see Sec. 4). If we assume a quadrupole misalignment of $\Delta x = 0.5$ mm, the error introduced by an error of $\Delta I = 0.1$ A for the compensation current is $G_1 \cdot \Delta I \cdot \Delta x \sim 0.004$ T.mm .

Additionally, beam position instabilities or drifts may introduce a significant error in the measurement. For control, we have recorded and compared the beam position measured upstream. Moreover, we have averaged the measured beam position over several pulses in order to minimize the error contribution from beam position jitter and BPM resolution. The estimated error from beam position jitter is in the order of a few percent.

8 Measurement of the scale calibration of quadrupole position sensors

The relative accuracy of the position sensors has been checked at quadrupole Q5UND2. We have inserted thin metal layers with thickness of 50 μm to 1 mm between the quadrupole Q5UND2 and its horizontal position sensor. The position readings from the sensor are shown in Fig. 10 as a function of the layer thickness. A linear fit to the measurement points gives a slope which differs by 4% from the ideal slope. For control, the sensor readings on the quadrupole surface have been recorded after each measurement point and plotted in Fig. 10 (horizontal line). The slope of the linear fit to the control points is 1% and gives an estimate of the reproducibility of the scale calibration.

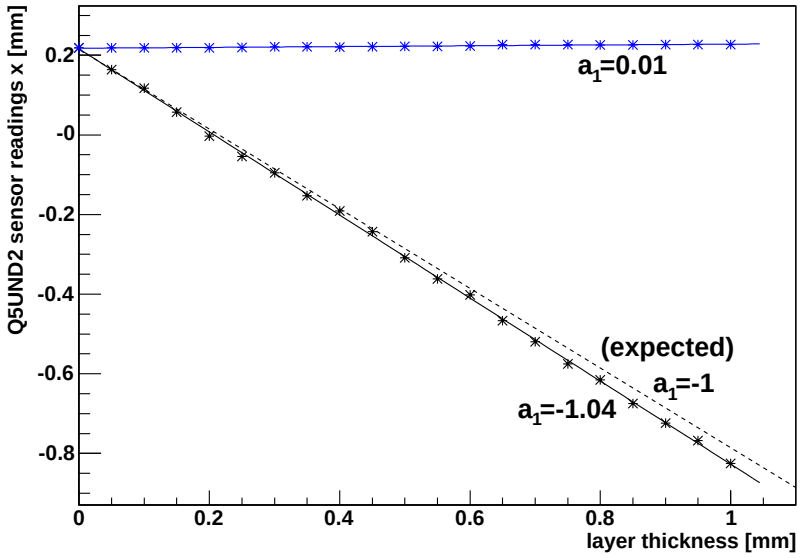

Figure 10: Readings of position sensor as a function of the thickness of the metal layer inserted (dark points). The blue points which lay horizontally are readings after the metal layer is removed (as control). The parameter a_1 is the slope of the line fitted.

9 Conclusions

We have used a method based on relative beam position measurements to measure the remanent dipole field in quadrupoles installed in the undulator section at FLASH. TQG quadrupoles have remanent dipole fields with an RMS amplitude of 0.08 T.mm and random direction. These fields deflect the beam trajectory in the undulator section and may cause an FEL gain reduction if not compensated. We recommend the use of the degausser in order to reduce the remanent fields to a minimum bias (as well as for the reproducibility of quadrupole fields).

However, the effect of remanent dipole fields on the beam is too weak to explain the strong horizontal beam deflection observed in the undulator section of about 0.41 T.mm in average per undulator segment (4.5 m) in the same direction [6]. This is corroborated by the fact that after degaussing all Q5 and Q6 quadrupoles the horizontal beam deflection is still present.

10 Acknowledgments

We would like to thank the FLASH team and the members of the TESLA Collaboration. Specially we would like to express our gratitude to Y. Holler and L. Gumprecht for their extensive efforts on magnetic measurements. Many thanks to J. Thomas for helping on measuring the scale calibration of quadrupole position sensors and to B. Faatz for his careful reading of this manuscript.

References

[1] The TESLA Test Facility FEL team; SASE FEL at the TESLA Facility, Phase 2, TESLA-FEL-2002-01.

[2] Y. Holler, L. Gumprecht, priv. communication.

[3] J. Pflüger, U. Hahn, B. Faatz, M. Tischer; Undulator system for the VUV FEL at the TESLA test facility phase-2, Nucl. Instr. Meth. A507 (2003) 228-233.

[4] V. Balandin, N. Golubeva; Commissioning 445 MeV optics for TTF2 linac: Towards choosing of a working point for the undulator quadrupoles, http://ttfinfo.desy.de/TTFelog/data/doc/Physics/Optics/2006-05-29T12:19:16-00.ps

[5] H. Wiedemann; Particle Accelerator Physics, Springer-Verlag, 1993.

[6] P. Castro; Beam trajectory investigations with degaussed quadrupoles in the undulator section in FLASH, TESLA-FEL-2006-10.